

Atmospheric Neutrinos: Status and Prospects

Sandhya Choubey^{1,2,*}

¹*Harish-Chandra Research Institute,*

Chhatnag Road, Jhansi, Allahabad 211 019, India

²*Department of Theoretical Physics,*

School of Engineering Sciences, KTH Royal Institute of Technology,

AlbaNova University Center, 106 91 Stockholm, Sweden

Abstract

We present an overview of the current status of neutrino oscillation studies at atmospheric neutrino experiments. While the current data gives some tantalising hints regarding the neutrino mass hierarchy, octant of θ_{23} and δ_{CP} , the hints are not statistically significant. We summarise the sensitivity to these sub-dominant three-generation effects from the next-generation proposed atmospheric neutrino experiments. We next present the prospects of new physics searches such as non-standard interactions, sterile neutrinos and CPT violation studies at these experiments.

arXiv:1603.06841v1 [hep-ph] 22 Mar 2016

*Electronic address: sandhya@hri.res.in

I. INTRODUCTION

In 1996, data from atmospheric neutrinos at the Super-Kamiokande (SK) experiment confirmed neutrino flavor oscillations beyond any doubt [1]. This established the existence of neutrino masses and mixing, and was hailed as the first unambiguous evidence of physics beyond the Standard Model (SM) of elementary particles. Finally, the year 2015 witnessed the awarding of Nobel Prize to Professor Takaaki Kajita for leading the SK collaboration to this remarkable discovery of flavor oscillation of atmospheric neutrinos. Professor Kajita shared the Nobel Prize with Professor Art McDonald of the Sudbury Neutrino Observatory, who was given the award for unambiguously establishing flavor oscillations of the solar neutrinos [2].

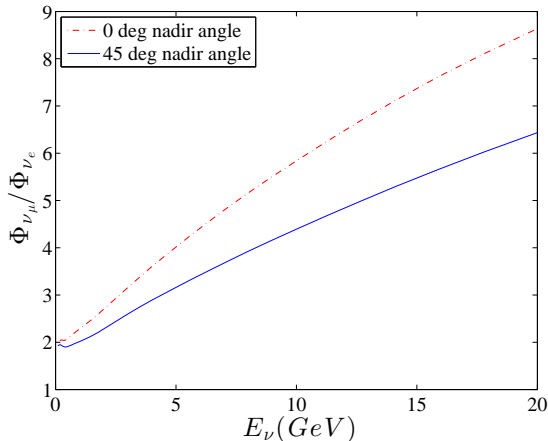


FIG. 1: Ratio of $\Phi_{\nu_\mu}/\Phi_{\nu_e}$ fluxes as a function of neutrino energy for two nadir angles of 0° and 45° .

Atmospheric neutrinos are produced when cosmic ray particles collide with the nuclei in the earth's atmosphere, producing pions and kaons which subsequently decay into neutrinos.

$$\begin{aligned}\pi^\pm &\rightarrow \mu^\pm + \nu_\mu(\bar{\nu}_\mu), \\ \mu^\pm &\rightarrow e^\pm + \bar{\nu}_\mu(\nu_\mu) + \nu_e(\bar{\nu}_e).\end{aligned}$$

We can see that these sets of decay channels would give the flux ratio of muon to electron neutrinos of about 2. The exact value of the atmospheric neutrino fluxes depend on a lot of issues and are calculated numerically for a given geographical location on earth [3]. We show

in Fig. 1 this ratio as a function of neutrino energy for two neutrino trajectories. The red broken line is for nadir angle of 0° (zenith angle 180°) and blue solid line is for nadir angle of 45° (zenith angle 135°). We note that this ratio is larger for more vertically traveling neutrinos and increases with increasing energy. The reason for the former is that the depth of the atmosphere is less for vertical trajectories compared to horizontal trajectories, giving vertically traveling particles lesser time to decay. The reason for the increase of this ratio with energy is that the higher energy particles take longer to decay making the decay process complete and leading to fewer electron type neutrinos and antineutrinos.

Atmospheric neutrinos were originally of interest to the high energy physics community mainly because they constituted the most significant background to proton decay experiments. Indeed, the first observation of atmospheric neutrinos was reported in 1965 at the Kolar Gold Field experiment in India [4] and almost simultaneously by an experiment led by Fred Reines in South Africa [5], both of which were looking for proton decay. A discrepancy between the predicted atmospheric neutrino fluxes and that observed in detectors was reported first by the Kamiokande II [6] experiment which was set-up to look for proton decay. This anomaly was resolved in terms of flavor oscillations by the SK experiment which established the existence of neutrino masses and mixing.

There are proposals to build bigger and better detectors in the future, some of which would be detecting atmospheric neutrinos. Amongst the most promising next-generation atmospheric neutrinos detectors are the Hyper-Kamiokande (HK) [7], which will be a megaton-class water Cherenkov detector with fiducial volume roughly 20 times that of SK. The ICAL detector at the India-based Neutrino Observatory (INO) [8] is proposed to be a 50 kton magnetised iron calorimeter. Being magnetised, this detector is expected to have very good charge identification efficiency. The Precision Icecube Next Generation Underground (PINGU) detector [9] is proposed as a low energy extension of the IceCube and is expected to have a fiducial volume in the multi-megaton range. This large volume makes this detector extremely promising. Along the same lines, with a very large fiducial volume is the ORCA proposal which will be the low energy extension of the KM3NeT detector in the Mediterranean [10].

In what follows, we will start with a brief discussion of the existing bounds from the SK atmospheric neutrino data in section 2. In section 3 we will discuss some important aspect of three-generation oscillations. Section 4 and 5 summarise the expected sensitivity

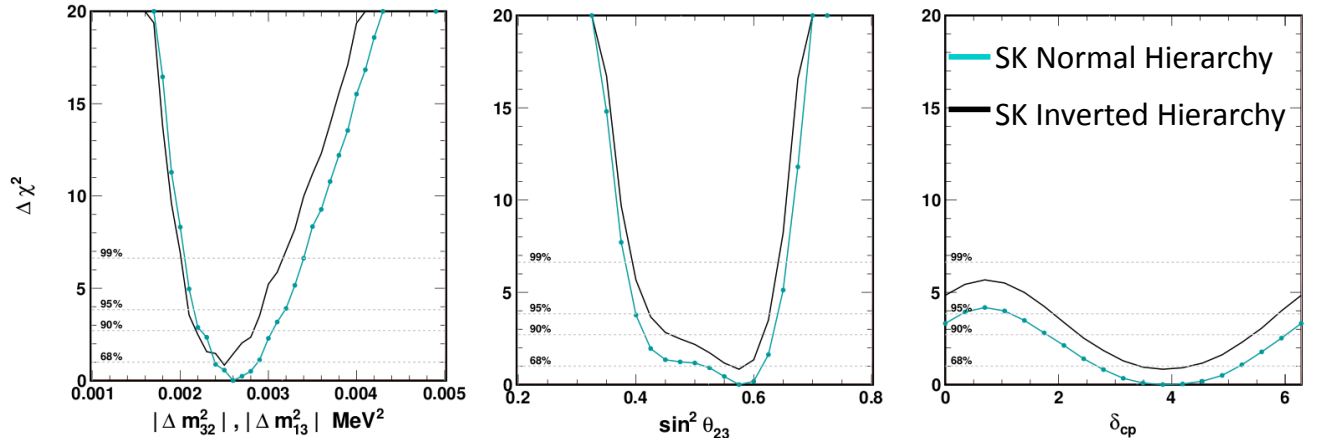


FIG. 2: Current limits from 4581.4 days SK data on atmospheric neutrinos. Reproduced from talk by Yoshinano Hayato on behalf of the SK collaboration, at WIN 2015, Germany.

from future experiments for neutrino mass hierarchy and octant of θ_{23} , respectively. We discuss bounds on non-standard interactions from atmospheric neutrinos in section 5, sterile neutrinos in section 6 and CPT violation in section 7. We finally conclude in section 8.

II. NEUTRINO OSCILLATIONS: ROLE OF ATMOSPHERIC NEUTRINOS SO FAR

The SK experiment until now has collected the most and the best data on atmospheric neutrinos. The detector is made of 50 kton of ultra-pure water with a fiducial volume of 22.5 kton, and started collecting data in April 1996. The entire data is divided into 4 sets called SKI, SKII, SKIII and SKIV, and the detector continues to operate. With 4581.4 days (282.2 kton-yrs) of data analysed, this is statistically overwhelming and we summarise the results in Fig. 2, (taken from talk by Yoshinano Hayato on behalf of the SK collaboration, at WIN 2015, Germany). The left and middle-panels of this figure show the constraint on the leading atmospheric neutrino oscillation parameters $|\Delta m_{31}^2|$ and $\sin^2 \theta_{23}$,

respectively. The right-panel shows the SK limits on the CP phase δ_{CP} . The colored lines are for normal hierarchy ($\Delta m_{31}^2 > 0$) while the black lines give the results for inverted hierarchy ($\Delta m_{31}^2 < 0$). We note that the difference in χ^2 between these two cases is not statistically significant. Therefore, this implies that the SK data is unable to resolve the sign of Δm_{31}^2 even though it can constrain its magnitude rather well (cf. left-panel). The weak results from the right-panel also indicates that SK is unable to make any statements about the CP phase δ_{CP} , though it does give a hint for $\delta_{CP} \simeq 230^\circ$. The middle-panel also indicates that the SK data prefers a value of θ_{23} which is non-maximal and also greater than $\pi/4$, however, this hint again is not necessarily consistent with other experiments and with global analyses of world neutrino data [11, 12] and will need confirmation from future experiments. In addition to SK, we also have recent results on atmospheric neutrinos from the MINOS [13] and IceCube DeepCore [14]. When combined with world neutrino data, the leading atmospheric neutrino parameters are constrained in the following 3σ range [11]

$$\begin{aligned}
+2.325 \times 10^{-3} &< \Delta m_{3l}^2/\text{eV}^2 < +2.599 \\
-2.59 \times 10^{-3} &< \Delta m_{3l}^2/\text{eV}^2 < -2.307 \\
0.385 &< \sin^2 \theta_{23} < 0.644,
\end{aligned}$$

where $l = 1$ for NH and $l = 2$ for IH. While the value of $|\Delta m_{31}^2|$ is mainly controlled by the long baseline data from T2K and MINOS, $\sin^2 \theta_{23}$ is mainly determined by the atmospheric neutrino data.

III. THREE-GENERATION PARADIGM AND THE SUBDOMINANT EFFECTS

Within the three-generation paradigm, the neutrino mass and mixing is parametrised in terms of 3 masses, 3 mixing angles and 3 CP phases, two of which are known as Majorana phases. They do not appear in the neutrino oscillations and show up only in lepton number violating processes such as neutrino-less double beta decay. Without them, the PMNS mixing matrix of the neutrinos is [15, 16] is parametrised as

$$U_{PMNS} = \begin{pmatrix} 1 & 0 & 0 \\ 0 & c_{23} & s_{23} \\ 0 & -s_{23} & c_{23} \end{pmatrix} \begin{pmatrix} c_{13} & 0 & s_{13}e^{-\delta_{CP}} \\ 0 & 1 & 0 \\ -s_{13}e^{-\delta_{CP}} & 0 & c_{13} \end{pmatrix} \begin{pmatrix} c_{12} & s_{12} & 0 \\ -s_{12} & c_{12} & 0 \\ 0 & 0 & 1 \end{pmatrix}. \quad (1)$$

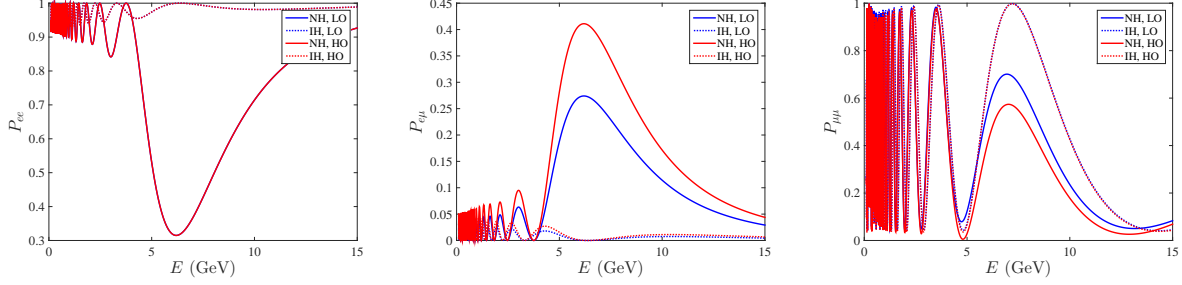


FIG. 3: Neutrino oscillation probabilities for a baseline of 7,000 km. The solid lines show the probabilities for $\Delta m_{31}^2 > 0$ and hence normal hierarchy (NH) while the broken lines are for $\Delta m_{31}^2 < 0$ and inverted hierarchy (IH). The blue lines are for $\sin^2 \theta_{23} = 0.4$ and hence Lower Octant (LO) while the red lines are for $\sin^2 \theta_{23} = 0.6$ and hence Higher Octant (HO). For the other oscillation parameters we use the following values: $\Delta m_{31}^2 = 2.5 \times 10^{-3} \text{ eV}^2$, $\Delta m_{21}^2 = 7.6 \times 10^{-5} \text{ eV}^2$, $\sin^2 \theta_{13} = 0.023$ and $\sin^2 \theta_{12} = 0.304$.

When neutrinos travel in matter their coherent forward charged current scattering off the ambient electrons leads to an extra effective contribution to the neutrino mass matrix [17–19]

$$H_f = \frac{1}{2E} U_{PMNS} \text{diag}(0, \Delta m_{21}^2, \Delta m_{31}^2) U_{PMNS}^\dagger + \text{diag}(A, 0, 0), \quad (2)$$

where $A = \pm\sqrt{2}G_F N_e$ is the effective matter potential [17–19], given in terms of the Fermi constant G_F and electron density in matter N_e . The sign of A is positive for neutrinos and negative for antineutrinos. It is seen that when GeV energy range atmospheric neutrinos travel inside the earth matter, they encounter sizeable changes due to the matter term which depends directly on the sign of Δm_{31}^2 and the value of θ_{13} . For $\theta_{13} = 0$, the matter effect is negligible, but since we now have very strong experimental evidence of $\sin^2 \theta_{13} \simeq 0.025$ from Daya Bay, RENO, Double Chooz, T2K, MINOS and NO ν A (see [11, 12] for a global analysis of data from all these experiments, and references therein), earth matter effects in atmospheric neutrinos are expected to be significant in the neutrino channel for $\Delta m_{31}^2 > 0$ and in the antineutrino channel for $\Delta m_{31}^2 < 0$.

While the SK atmospheric data has confirmed the leading $|\Delta m_{31}^2|$ -driven flavor oscillations beyond doubt, the subdominant effects coming from the three-generation paradigm remains to be confirmed, as was discussed in the previous section. The most important issues on which the data from future atmospheric neutrino experiments could throw light are the issue

of the sign of Δm_{31}^2 , *aka*, the neutrino mass hierarchy or the neutrino mass ordering [20–38] and the correct octant of θ_{23} [39–42] meaning whether $\theta_{23} < \pi/4$ or $> \pi/4$. In addition, these experiments could also play a role in CP studies [43–46] at long baseline experiments which suffer due to their lack of knowledge of the mass hierarchy. In most cases, its mainly the presence of the θ_{13} -driven earth matter effects which give atmospheric neutrinos the handle to probe these issues, although sometimes Δm_{21}^2 -driven subdominant oscillations are also instrumental in the diagnostics.

We show in Fig. 3 the neutrino oscillation probabilities as a function of the neutrino energies for the earth mantle crossing neutrino trajectory corresponding to a baseline of $L = 7000$ km. The solid lines show the probabilities for $\Delta m_{31}^2 > 0$ and hence normal hierarchy (NH) while the broken lines are for $\Delta m_{31}^2 < 0$ and inverted hierarchy (IH). The blue lines are for $\sin^2 \theta_{23} = 0.4$ and hence Lower Octant (LO) while the red lines are for $\sin^2 \theta_{23} = 0.6$ and hence Higher Octant (HO). We see that the probabilities are distinctly different between the NH and IH as well as between LO and HO cases. In both cases, its the earth matter effects which bring in the major difference between NH vs IH as well as LO vs HO. For the electron neutrino survival probability P_{ee} there is no effect of θ_{23} since it does not depend on this parameter, but shows a sharp dependence on the mass hierarchy. The muon neutrino survival probability $P_{\mu\mu}$ changes both due to hierarchy as well as θ_{23} octant, however, the octant effect shows up only for the mass hierarchy case which develops earth matter effects. In addition, the difference between the probability corresponding to NH and IH also changes sign as we change neutrino energy E (as can be seen from Fig. 3) as well as L (for which one has to do this figure for another baseline). The earth matter effects seen in the conversion probability $P_{e\mu}$ from ν_e to ν_μ shown in the middle panel depends on the octant and does not change sign with L and E . From the discussion above we conclude that in order to see earth matter effects in muons through $P_{\mu\mu}$ one needs a detector with good energy and angle (and hence L) resolution. On the other hand, these requirements are not mandatory in detectors which can observe electrons and measure P_{ee} . However, $P_{\mu\mu}$ also brings in information on octant while P_{ee} does not. The conversion channel $P_{e\mu}$ is required for both the muon as well as electron channels.

IV. NEUTRINO MASS HIERARCHY

Discovery of the neutrino mass hierarchy is the next major goal in the field of neutrino physics. Mass hierarchy sensitivity is given in terms of the difference between the signal at the detector between the NH and IH cases. Experiments such as INO, PINGU and ORCA are being proposed with the main goal of determining the neutrino mass hierarchy. Mass hierarchy determination studies at atmospheric neutrino experiments need to face the challenge coming from two major screening effects which reduce the sensitivity of these experiments. We discuss them briefly below.

The first challenge comes from the fact that matter effects develop only in the neutrino ($N_\alpha(\text{matter})$) or the antineutrino channel ($N_{\bar{\alpha}}(\text{matter})$) for a given true hierarchy. However, both neutrinos as well as antineutrinos come mixed together in the atmospheric neutrinos flux at the detector. For experiments which can distinguish between the charge of the final state lepton such as the magnetised ICAL detector at INO, this challenge does not pose any significant problem. On the other hand, for detectors which can't determine the charge of the particle, this complication does result in reducing the sensitivity to measuring earth matter effects and hence mass hierarchy. Since the total events recorded at the detector for NH is roughly given by $N_\alpha(\text{matter}) + N_{\bar{\alpha}}$ and for IH is $N_\alpha + N_{\bar{\alpha}}(\text{matter})$, the mass hierarchy sensitivity can be estimated in terms of the difference

$$\begin{aligned} \Delta N &\simeq (N_\alpha(\text{matter}) + N_{\bar{\alpha}}) - (N_\alpha + N_{\bar{\alpha}}(\text{matter})) \\ &\simeq (N_\alpha(\text{matter}) - N_{\bar{\alpha}}(\text{matter})) + (N_{\bar{\alpha}} - N_\alpha), \end{aligned}$$

where N_α and $N_{\bar{\alpha}}$ are the number of events in the neutrino and antineutrino channel of flavor α , and we have assumed that there is no effect of matter for the neutrino (antineutrinos) for NH (IH), which is not a bad assumption. If the atmospheric neutrino flux was same for neutrinos and antineutrinos of all flavors, and if the interaction cross-section of the neutrinos were same as the interaction cross-section of the antineutrinos then the number of events for neutrinos and antineutrinos would be identically same. In that case $N_\alpha(\text{matter}) = N_{\bar{\alpha}}(\text{matter})$ and $N_{\bar{\alpha}} = N_\alpha$ and $\Delta N = 0$, washing out completely the mass hierarchy sensitivity. However, this does not happen because even though at the probability level the matter effect in the neutrino channel for NH is the same as the matter effect in the antineutrino channel for IH, the fluxes of neutrinos are different from the fluxes of the

antineutrinos, and more importantly, the neutrino-nucleon cross-sections are lower for the anti-neutrinos than for the neutrinos. Therefore, even detectors with no charge identification capability can be sensitive to the neutrino mass hierarchy.

The next level of difficulty due to screening of earth matter effects in atmospheric neutrinos comes from the fact the atmospheric neutrinos come in both muon as well as electron flavors. Therefore, if one is observing the ν_μ signal in the detector, the final fluxes are a combination of the survived ν_μ flux (disappearance channel) and the oscillated ν_e flux (appearance channel). The net flux at the detector is a combination of the original fluxes folded with the relevant oscillation probabilities. For instance, the net ν_μ flux at the detector is given by

$$\Phi_{\nu_\mu} = \Phi_{\nu_\mu}^0 P_{\mu\mu} + \Phi_{\nu_e}^0 P_{e\mu}, \quad (3)$$

where $\Phi_{\nu_\mu}^0$ and $\Phi_{\nu_e}^0$ are the fluxes before oscillations. A quick look at Fig. 3 reveals that while matter effect reduces $P_{\mu\mu}$ for the neutrinos for NH, it increases $P_{e\mu}$. Therefore, the net impact of matter effects in atmospheric neutrinos get partially washed down by adding the so-called appearance channel ($\Phi_{\nu_e}^0 P_{e\mu}$) to the disappearance channel ($\Phi_{\nu_\mu}^0 P_{\mu\mu}$). Again, $\Phi_{\nu_\mu}^0 / \Phi_{\nu_e}^0 \simeq 2$ for lower energies and higher for higher energies, the cancellation is not complete and the residual matter effects can be used to probe the neutrino mass hierarchy.

The most promising next generation atmospheric neutrino experiments that could throw light on the mass hierarchy are PINGU, HK, INO and ORCA. All of these detectors are planned to be large and can observe earth matter effects to different degrees of efficiency. While INO has excellent charge identification capabilities, PINGU, ORCA and HK are very big in size. In addition, the water and ice detectors are also sensitive to electrons and hence can probe the mass hierarchy in both channels. All of these experiments have made available their mass hierarchy sensitivity. The χ^2 quoted have been calculated as follows. Data was generated at certain assumed true mass hierarchy and with a certain assumed set of values for the other oscillation parameters. This is then fitted with the other hierarchy allowing the oscillation parameters to vary in the fit and picking out the smallest χ^2 value from the set. We give the number of years of data in a given experiment to reach $\chi^2 = 9$ and we do this for both hierarchies assumed as true. Since the values of θ_{13} as well as θ_{23} directly impacts the projected sensitivity and since the sensitivity increases with the increase of both these mixing angles, we also mention the values of these mixing angles used in the

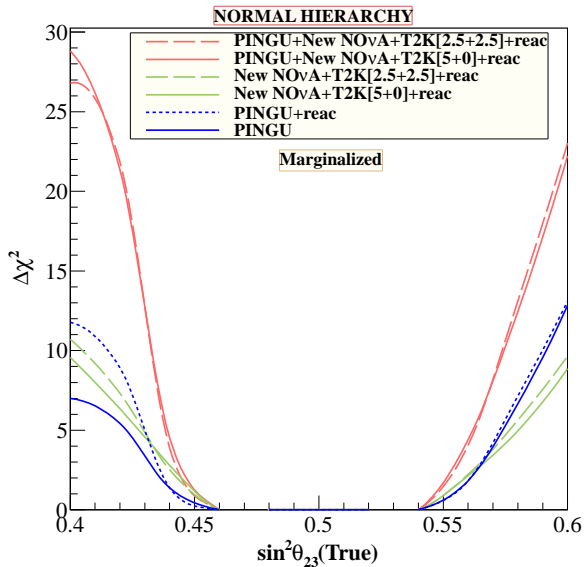


FIG. 4: $\Delta\chi^2$ as a function of $\sin^2\theta_{23}(\text{true})$ for the wrong octant from 3 years of atmospheric neutrino data from PINGU combined with data from 3+3 years of running of NO ν A, 5+0 years of running OR 2.5+2.5 years of running of T2K and 3 years of running of Daya Bay, RENO and Double Chooz. The true hierarchy was assumed to be NH. Reproduced from [42].

relevant study from which these results have been quoted. For NH true and $\sin^2 2\theta_{13} = 0.08$ and $\sin^2\theta_{23} = 0.5$, HK gives a $\chi^2 = 9$ with about 4.5 years of data. PINGU promises to give a $\chi^2 = 9$ for the wrong mass hierarchy with about 3 years of data for NH true. On the other hand INO being a much smaller detector would need about 8.5 years of data for $\chi^2 = 9$ when $\sin^2 2\theta_{13} = 0.1$ and $\sin^2\theta_{23} = 0.5$ for NH true. However, if one compares the sensitivity expected for true IH, it is seen that while the sensitivity of both HK and PINGU go down significantly, the sensitivity for INO remains almost the same as in the true NH case. The main reason for this is that INO has excellent charged identification capabilities which returns nearly the same sensitivity. On the other hand HK and PINGU suffer due to the partial washing down of the matter effects by mixing of the neutrino and antineutrino signal¹.

¹ See [42] for a detailed discussion on a similar issue concerning the decrease in the octant sensitivity of PINGU.

V. OCTANT OF θ_{23}

We have seen in Fig. 3 that the earth matter effects in the muon neutrino survival probability has a θ_{23} dependence. This gets diluted due to the presence of the appearance channel as was also discussed in the earlier section on mass hierarchy. However, the residual dependence that remains in the muon data can be used to constrain θ_{23} and find its octant. To illustrate the sensitivity of atmospheric neutrinos to the octant of θ_{23} , we show in Fig. 4 the sensitivity of the PINGU experiment. The figure shows the $\Delta\chi^2$ obtained by generating the data for a given true value of $\sin^2\theta_{23}$ shown in the x-axis and fitting it with values of $\sin^2\theta_{23}$ in the entire wrong octant side and picking out the best fit. The blue solid line shows the sensitivity of 3 years of PINGU alone, while the blue broken line shows the sensitivity when the reactor data is added to PINGU data. The green lines show the comparative sensitivity expected from the T2K and NO ν A experiments which are seen to have a sensitivity comparable to that of PINGU. For NO ν A the simulation uses the fluxes and run times given in their DPR while for T2K 2 cases are displayed, one with 5 years of neutrino running alone and another with 2.5 years of neutrino and 2.5 years of antineutrino running. Finally, the red lines show the combined χ^2 obtained when we add the T2K, NO ν A and reactor data to the data from 3 years of PINGU. The χ^2 for all cases is marginalised over Δm_{31}^2 and $\sin^2\theta_{13}$ and for T2K and NO ν A we also marginalise over δ_{CP} . The figure was generated for NH as true and a similar figure for IH can be found in [42]. The sensitivity for IH is a little lower and is explained in [42].

VI. NON-STANDARD INTERACTIONS

It is now well established that the standard model of particle physics (SM) needs to be extended. Most of such extensions of the SM involve addition of new particles and/or extension of the gauge sector. The low energy limit of such theories can be expected to have effective couplings which are different from that given in the SM. These effective couplings could give rise to additional charged current interactions as well as neutral current interactions and are in general referred to as Non-Standard Interactions (NSI) [17, 47–50]. The additional charged interactions due to new physics would show up in the production and detection of the neutrinos, while the neutral current interaction could significantly impact

the neutrino propagation inside matter. The couplings that drive the additional charged current interactions of the neutrinos will also lead to corresponding beyond SM interactions in the charged lepton sector due to the $SU(2)_L$ symmetry of the SM. These couplings are therefore severely constrained from existing data [51]. On the other hand, constraints on the neutral current couplings are less and have been calculated to be [51]

$$|\epsilon_{\alpha\beta}| < \begin{pmatrix} 4.2 & 0.33 & 3.0 \\ 0.33 & 0.068 & 0.33 \\ 3.0 & 0.33 & 21 \end{pmatrix}, \quad (4)$$

where the parameters have been arranged in the form of a matrix with the rows and columns corresponding to $\{e, \mu, \tau\}$ and the bounds are obtained at the 90% C.L.. We note that the bounds on some of the parameters are rather weak. In particular the bound on $\epsilon_{\tau\tau}$ looks very loose. These bounds are called indirect bounds in the literature since they are derived from non-neutrino-oscillation experimental data. These parameters also affects the propagation of neutrinos in matter through effective operators. In particular, within the framework of an effective two-generation hybrid model, the SK collaboration has put a 90% C.L. limit on the parameter $\epsilon_{\mu\tau} < 0.033$ and $|\epsilon_{\tau\tau} - \epsilon_{\mu\mu}| < 0.147$ [52, 53]. A comparison with Eq. (4) shows that neutrino experiments have much better handle on these parameters and an attempt to look at the potential on future experiments to constrain these parameters is pertinent. Here we review the prospects of atmospheric neutrino experiments in constraining these NSI. In addition, since the source-detector NSI are very severely constrained while matter NSI are still loosely bounded, in what follows we will discuss the current and expected bounds coming from the matter NSI only. A lot of work has been done in this field (for illustration, see [54–66] and references therein)

The neutrino oscillation probabilities change in the presence of NSI. The neutrino oscillation probabilities in the framework on three-generations of neutrinos and in presence of NSI were calculated in [67]. Keeping first order terms in the (small) NSI parameters and zeroth terms in $\Delta m_{21}^2/\Delta m_{31}^2$ and $\sin^2 \theta_{13}$ one obtains the difference in the probabilities [62, 67]

$$\Delta P_{\mu\mu} = P_{\mu\mu}^{\text{NSI}} - P_{\mu\mu}^{\text{SM}} \quad (5)$$

$$\begin{aligned} &\simeq -|\epsilon_{\mu\tau}|c_{\phi_{\mu\tau}}\bar{A} [\sin^3(2\theta_{23})\Delta \sin(\Delta) + 4 \sin(2\theta_{23}) \cos^2(2\theta_{23}) \sin^2(\Delta/2)] \\ &+ (|\epsilon_{\mu\mu}| - |\epsilon_{\tau\tau}|)\bar{A} \sin^2(2\theta_{23}) \cos(2\theta_{13}) [\Delta \sin(\Delta)/2 - 2 \sin^2(\Delta/2)], \quad (6) \end{aligned}$$

where $\Delta \equiv \Delta m_{31}^2 L / (2E)$, $\bar{A} \equiv \sqrt{2} G_F N_e E / \Delta m_{31}^2 = A / \Delta m_{31}^2$, where A is the matter potential defined before. A similar expression can be obtained for the other oscillation parameters, ΔP_{ee} and $\Delta P_{e\mu}$, however, we do not give them here for the sake of brevity.

As can be seen from Eq. (6), the muon neutrino survival probability predominantly depends on the NSI parameters $\epsilon_{\mu\tau}$ and $|\epsilon_{\tau\tau} - \epsilon_{\mu\mu}|$. Likewise the conversion channel $P_{e\mu}$ primarily depends on the NSI parameters $\epsilon_{e\mu}$ and $\epsilon_{e\tau}$. Constraints on matter NSI from existing atmospheric data have been studied in [54–59, 61, 65]. The NSI parameters are expected to be much better constrained in future atmospheric neutrino experiments using bigger and better detectors. With three years of data, we expect the following constraints on the leading NSI parameters from PINGU 90% C.L.(3σ) for NH [62]

$$\begin{aligned} -0.0043 \text{ } (-0.0048) &< \epsilon_{\mu\tau} < 0.0047 \text{ } (0.0046), \\ -0.03 \text{ } (-0.016) &< \epsilon_{\tau\tau} < 0.017 \text{ } (0.032), \end{aligned}$$

while INO with 10 years of data could give the following constraints at 90% C.L.(3σ) for NH [66]

$$\begin{aligned} -0.12 \text{ } (-0.28) &< \epsilon_{e\mu} < 0.104 \text{ } (0.23), \\ -0.13 \text{ } (-0.3) &< \epsilon_{e\tau} < 0.102 \text{ } (0.21), \\ -0.015 \text{ } (-0.027) &< \epsilon_{\mu\tau} < 0.015 \text{ } (0.027), \\ -0.07 \text{ } (-0.104) &< \epsilon_{\tau\tau} < 0.07 \text{ } (0.104). \end{aligned}$$

The limits for IH come out to be similar.

As discussed above, one of the major physics goals of the atmospheric neutrino experiments is to determine the neutrino mass hierarchy. For this what is relevant is the difference in the neutrino oscillation probabilities between NH and IH which is mainly driven by earth matter effects. The presence of matter NSI modifies the effective interaction of the neutrinos with matter, changing the earth matter effect and hence the oscillation probabilities. This change is different for the two mass hierarchies. The difference in the neutrino oscillation probabilities between NH and IH in presence of NSI parameters has been discussed in [62–64] and studied in details in [66] in the context of INO. We show in Fig. 5 the effect of NSI parameters on the mass hierarchy sensitivity of INO. This figure gives the χ^2 when the data is generated for a given neutrino mass hierarchy and a non-zero value of the NSI parameter

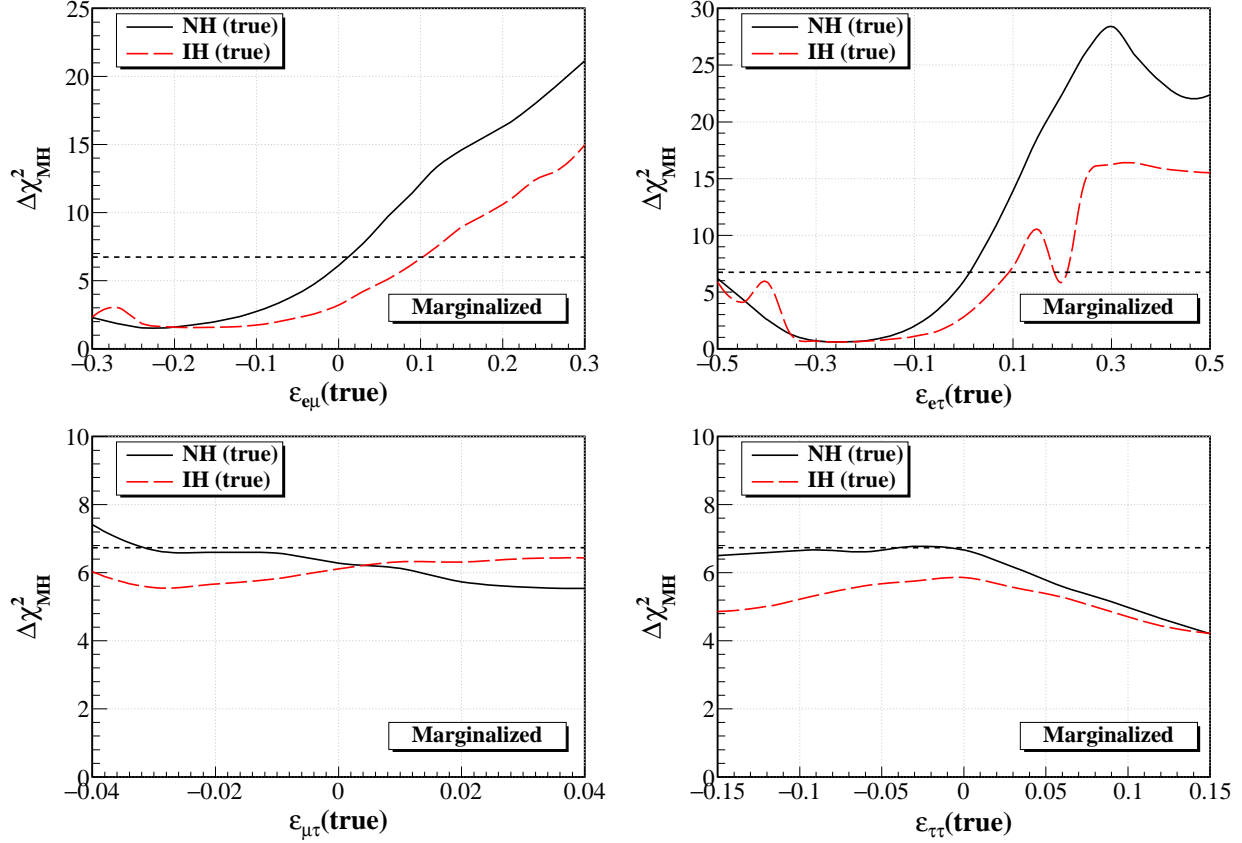


FIG. 5: The $\Delta\chi^2_{\text{MH}}$, giving the expected mass hierarchy sensitivity from 10 years of running of INO, as a function of the true value of NSI parameters. We keep only one $\epsilon_{\alpha\beta}(\text{true})$ to be non-zero at a time, while others are set to zero. The $\Delta\chi^2$ is obtained after marginalisation over the oscillation parameters. Reproduced from [66].

and the fitted with the wrong hierarchy. The corresponding χ^2 is plotted as a function of the NSI parameter value used in the data. Only one NSI parameter is taken in the data at a time for simplicity. The figure shows that the mass hierarchy sensitivity does change in presence of NSI parameters $\epsilon_{e\mu}$ and $\epsilon_{e\tau}$, while $\epsilon_{\mu\tau}$ and $\epsilon_{\tau\tau}$ do not affect it much.

VII. PROBING STERILE NEUTRINOS

The decay width of the Z boson measured at LEP restricts the number of light neutrino species which couple to the Z boson to be very close to 3. Hence any light neutrino species beyond the already known three neutrinos should not have any gauge interactions and are

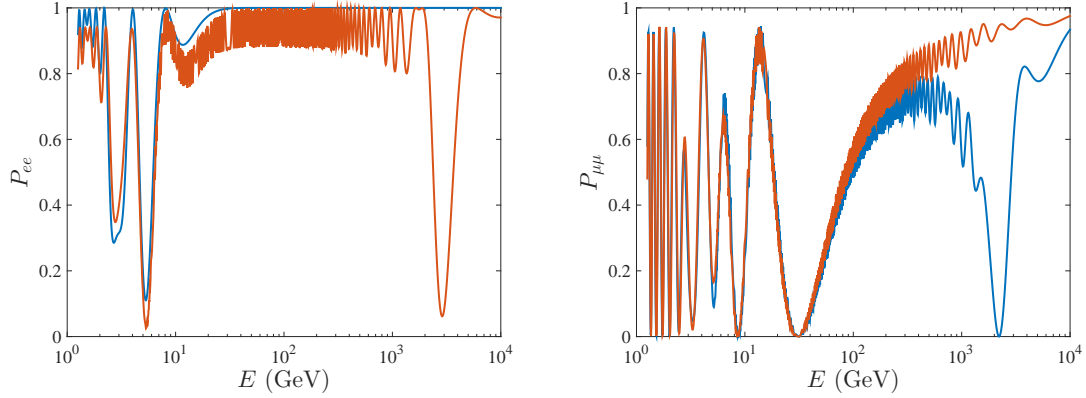


FIG. 6: Neutrino oscillation probabilities in the 3+1 scenario with 1 extra sterile species for the earth centre crossing trajectory. The red lines show the survival probabilities with mass squared difference $\Delta m_{41}^2 = -1.0 \text{ eV}^2$ while the blue lines are for $\Delta m_{41}^2 = 1.0 \text{ eV}^2$. All the sterile mixing angles θ_{14} , θ_{24} and θ_{34} are taken at a benchmark value of 10° . For the other oscillation parameters we use the same values as in Fig. 3.

hence known as sterile neutrinos. These additional sterile neutrinos have been postulated as a possible explanation of the excess observed at the LSND [68] and MiniBooNE [69] experiments. In addition to the LSND (and MiniBooNE) hints, we also have the reactor anomaly wherein the measured reactor anti-neutrino fluxes are found to be lower than that predicted by the theory [70, 71], and again this discrepancy can be explained by flavor oscillations of sterile neutrinos. A variety of accelerator and reactor based experiments have been proposed to verify these two anomalies and to confirm or disprove the existence of sterile neutrinos.

Presence of sterile neutrino species is also expected to alter the flavor oscillations of atmospheric neutrinos. This change is brought about due to two reasons. Firstly the active-sterile mass squared difference is postulated to be in the 1 eV^2 regime. This would give rise to very fast oscillations of GeV-range neutrinos, and would lead to flavor oscillations of downward neutrinos, which in the three-flavor set-up remain unaffected. Secondly, while all active neutrino species undergo neutral current scattering over the ambient earth matter, the sterile neutrinos do not interact. This leads to neutral current driven matter effects which changes the neutrino mass and mixing inside the earth matter and hence oscillation probabilities.

In Fig. 6 we show the neutrino oscillation probabilities as a function of the neutrino energies for the earth centre crossing neutrino trajectory ($L = 2R_e$, where R_e is the radius of the earth) in the so-called 3+1 framework, where we add 1 extra sterile neutrinos to the 3 active ones. The mixing matrix is likewise extended to become 4×4 and for this figure we have used the parametrisation

$$U_{4gen} = R(\theta_{34})R(\theta_{24})R(\theta_{23})R(\theta_{13})R(\theta_{12}), \quad (7)$$

where R_{ij} are the rotation matrices and θ_{ij} the corresponding mixing angle. For neutrino traveling in matter there comes in a further contribution to the flavor mixing from the neutral current scattering since while the active flavors all undergo (equal) amount of coherent forward scattering, the sterile species remain unaffected. Thus the neutrino mass matrix in matter for sterile neutrinos is extended to

$$H_f = \frac{1}{2E}U_{4gen} \text{diag}(0, \Delta m_{21}^2, \Delta m_{31}^2, \Delta m_{41}^2) U_{4gen}^\dagger + \text{diag}(A, 0, 0, 0) + \text{diag}(0, 0, 0, A_{NC}), \quad (8)$$

where $A_{NC} = \pm\sqrt{2}G_F N_n/2$ and we have subtracted out the common neutral current components from the active sector leaving behind the term in the sterile part. In the way we have written, A_{NC} is positive for neutrinos and negative for antineutrinos. Just like in the case of A , we encounter matter enhanced resonance due to A_{NC} as well, as can be seen in the Fig. 6. However, unlike the case of active neutrinos, the resonance for sterile neutrinos occurs in the ν_μ sector for $\Delta m_{41}^2 < 0$ and in the $\bar{\nu}_\mu$ sector for $\Delta m_{41}^2 < 0$. This is because in the effective two-generation approximation, the resonance condition for the muon neutrinos is given by $A_{NC} = -\Delta m_{41}^2 \cos \theta_{24}$. For the ν_e the resonance condition is $A - A_{NC} = \Delta m_{41}^2 \cos \theta_{14}$ and hence continues to occur for ν_e when $\Delta m_{41}^2 > 0$ and for $\bar{\nu}_e$ when $\Delta m_{41}^2 < 0$, since $A_{NC} \simeq A/2$.

From the figure, we see that the earth matter effects changes the muon neutrino survival probability somewhat in the energy range 1-100 GeV. This energy range can be probed in detectors like SK, INO, PINGU and ORCA. The analysis of the current SK data confirms the three-flavor paradigm and constrains the sterile neutrino mass and mixing. An analysis of the 4438 days of SK atmospheric neutrino data restricts the active-sterile neutrino mixing to $|U_{\mu 4}|^2 < 0.041$ and $|U_{\tau 4}|^2 < 0.18$ for $\Delta m_{41}^2 > 0.1 \text{ eV}^2$ at the 90% C.L. in the 3+1 scenario [72].

However, as Fig. 6 shows, very dramatic effects appear in the oscillation probabilities for the energy range of 100 GeV to 10 TeV, where we witness resonant oscillations due to the

sterile neutrino Δm^2 -driven matter resonance. This dramatic effect on atmospheric neutrino fluxes in the TeV energy range has been studied in detail in [73–75]. It was pointed out that the TeV atmospheric neutrino events recorded in IceCube can be used to constrain the sterile neutrino mass and mixing plane. There have been attempts to analyse the IceCube data to constrain the sterile neutrino mixing by looking for the sharp change in the expected track to shower ratio at IceCube [76–80].

VIII. CPT VIOLATION STUDIES

Lorentz and CPT invariance are one the basic postulates of modern day quantum field theory. However, motivated partly by string theories and other attempted quantum theories of gravity, there have been some interest in looking for breakdown of these symmetries at the Plank scale. While a discussion of these theories is outside the scope of this article, we will here look at some of the phenomenological implications for atmospheric neutrinos if CPT and/or Lorentz invariance is indeed violated. As effective field theory which includes all features of the standard model as well as all possible Lorentz violating terms was proposed by Kostelecky and Mewes and goes by the name Effective Standard-Model Extension (SME) [81, 82]. However, most studies on neutrino oscillations use a more phenomenological approach wherein a few Lorentz violating terms are added to the standard model Lagrangian. For example, many studies add to the standard Lagrangian an effective CPT violating term parametrised as

$$\mathcal{L}_\nu^{\text{CPTV}} = \bar{\nu}_L^\alpha b_{\alpha\beta}^\mu \gamma_\mu \nu_L^\beta \quad (9)$$

where the Lorentz and CPT is explicitly seen to be violated by the 3×3 Hermitian matrices which carry the bare Lorentz index μ and flavor indices α and β . The only surviving CPTV component is $b_{\alpha\beta}^0$. The form of this term is similar to that of the matter potential and results in changing the dispersion relation of the neutrinos in vacuum to

$$H = \frac{MM^\dagger}{2p} + b^0 \quad (10)$$

where M is the neutrino mass matrix and b^0 is a 3×3 non-diagonal matrix. Atmospheric neutrinos also travel in matter and therefore the neutrino Hamiltonian in matter in presence of CPTV written in the flavor basis is given by

$$H_f = \frac{1}{2E} U_{PMNS} \text{diag}(0, \Delta m_{21}^2, \Delta m_{31}^2) U_{PMNS}^\dagger + U_b \text{diag}(0, \delta b_{21}, \delta b_{31}) U_b^\dagger + \text{diag}(A, 0, 0) \quad (11)$$

where $\delta b_{ij} = b_i - b_j$ and U_b is the matrix which diagonalises b^0 giving eigenvalues b_i , and the other quantities are as defined in the previous sections. The mixing matrix U_b has 3 angles and 3 phases, all of which are physical while U_{PMNS} has 3 angles and 1 phase. Considering the most general case with these 6 mixing angles, 4 phases and 4 independent eigenvalues parametrised as Δm_{21}^2 , Δm_{31}^2 , δb_{21} and δb_{31} can be challenging. However attempts have been made in the literature to study the impact of CPTV on atmospheric neutrinos (see [83] and references therein).

In [83], the authors studied the effect of CPTV in atmospheric signals in detectors like INO which have charge identification capabilities. The possibility of separating the neutrino from anti-neutrino signals at these detectors give them an added handle in containing these CPTV parameters. From a χ^2 analysis of the expected 10 years data from INO, the authors [83] determine that INO could restrict $\delta b_{31} \gtrsim 4 \times 10^{-23}$ GeV at the 99% C.L. for both types of neutrino mass hierarchies, while the constraints on δb_{21} are not competitive with other experiments.

IX. CONCLUSIONS

Atmospheric neutrinos detected in SK were the first to give unambiguous evidence of neutrino oscillations and hence the first solid evidence for physics beyond the standard model. This landmark achievement was acknowledged by honouring Prof. Kajita of the SK experiment with the Nobel Prize in 2015. The data collected at SK still is a driving force in global analyses. It also provides some hints regarding the as-of-yet unknowns in neutrino physics, such as the octant of θ_{23} , δ_{CP} and to a small extent the mass hierarchy. All of these parameters play a sub-dominant role in the three-generation oscillation probabilities relevant for atmospheric neutrinos.

A variety of next generation atmospheric neutrinos detectors such as the HK, PINGU, ORCA and INO have to been proposed to catch some of these sub-leading aspects, particularly the neutrino mass hierarchy. In this article, we have discussed the expected reach of these future experiments towards discovery of the true mass hierarchy and octant of θ_{23} . We have also discussed the importance of atmospheric neutrinos in probing new physics such as presence of sterile neutrinos, NSI and CPT violation. Atmospheric neutrino experiments indeed could continue to play a crucial role in the field of neutrino physics in the years to

come.

Acknowledgments

SC acknowledge support from the Neutrino Project under the XII plan of Harish-Chandra Research Institute and partial support from the European Union FP7 ITN INVISIBLES (Marie Curie Actions, PITN-GA-2011-289442)

-
- [1] Y. Fukuda et al. (Super-Kamiokande), Phys. Rev. Lett. **81**, 1562 (1998), hep-ex/9807003.
 - [2] Q. R. Ahmad et al. (SNO), Phys. Rev. Lett. **89**, 011301 (2002), nucl-ex/0204008.
 - [3] M. Honda, T. Kajita, K. Kasahara, and S. Midorikawa, Phys. Rev. **D70**, 043008 (2004), astro-ph/0404457.
 - [4] C. V. Achar et al., Phys. Lett. **18**, 196 (1965).
 - [5] F. Reines, M. F. Crouch, T. L. Jenkins, W. R. Kropp, H. S. Gurr, G. R. Smith, J. P. F. Sellschop, and B. Meyer, Phys. Rev. Lett. **15**, 429 (1965).
 - [6] K. S. Hirata et al. (Kamiokande-II), Phys. Lett. **B205**, 416 (1988), [,447(1988)].
 - [7] E. Kearns et al. (Hyper-Kamiokande Working Group), in *Community Summer Study 2013: Snowmass on the Mississippi (CSS2013) Minneapolis, MN, USA, July 29-August 6, 2013* (2013), 1309.0184, URL <http://inspirehep.net/record/1252067/files/arXiv:1309.0184.pdf>.
 - [8] S. Ahmed et al. (ICAL) (2015), 1505.07380.
 - [9] M. Aartsen et al. (IceCube-PINGU Collaboration) (2014), 1401.2046.
 - [10] S. Adrian-Martinez et al. (KM3Net) (2016), 1601.07459.
 - [11] M. C. Gonzalez-Garcia, M. Maltoni, and T. Schwetz (2015), 1512.06856.
 - [12] F. Capozzi, E. Lisi, A. Marrone, D. Montanino, and A. Palazzo (2016), 1601.07777.
 - [13] P. Adamson et al. (MINOS), Phys. Rev. Lett. **112**, 191801 (2014), 1403.0867.
 - [14] M. Aartsen et al. (IceCube), Phys. Rev. **D91**, 072004 (2015), 1410.7227.
 - [15] Z. Maki, M. Nakagawa, and S. Sakata, Prog. Theor. Phys. **28**, 870 (1962).
 - [16] B. Pontecorvo, Sov. Phys. JETP **7**, 172 (1958), [Zh. Eksp. Teor. Fiz.34,247(1957)].
 - [17] L. Wolfenstein, Phys. Rev. **D17**, 2369 (1978).

- [18] S. P. Mikheev and A. Yu. Smirnov, *Nuovo Cim.* **C9**, 17 (1986).
- [19] S. P. Mikheev and A. Yu. Smirnov, *Sov. J. Nucl. Phys.* **42**, 913 (1985), [*Yad. Fiz.*42,1441(1985)].
- [20] J. Bernabeu, S. Palomares-Ruiz, A. Perez, and S. T. Petcov, *Phys. Lett.* **B531**, 90 (2002), hep-ph/0110071.
- [21] M. C. Gonzalez-Garcia and M. Maltoni, *Eur. Phys. J.* **C26**, 417 (2003), hep-ph/0202218.
- [22] J. Bernabeu, S. Palomares Ruiz, and S. T. Petcov, *Nucl. Phys.* **B669**, 255 (2003), hep-ph/0305152.
- [23] S. Palomares-Ruiz and S. T. Petcov, *Nucl. Phys.* **B712**, 392 (2005), hep-ph/0406096.
- [24] D. Indumathi and M. V. N. Murthy, *Phys. Rev.* **D71**, 013001 (2005), hep-ph/0407336.
- [25] R. Gandhi, P. Ghoshal, S. Goswami, P. Mehta, and S. U. Sankar, *Phys. Rev.* **D73**, 053001 (2006), hep-ph/0411252.
- [26] S. T. Petcov and T. Schwetz, *Nucl. Phys.* **B740**, 1 (2006), hep-ph/0511277.
- [27] S. Choubey, *Nucl. Phys. Proc. Suppl.* **221**, 46 (2011), hep-ph/0609182.
- [28] E. K. Akhmedov, M. Maltoni, and A. Yu. Smirnov, *JHEP* **05**, 077 (2007), hep-ph/0612285.
- [29] R. Gandhi, P. Ghoshal, S. Goswami, P. Mehta, S. U. Sankar, and S. Shalgar, *Phys. Rev.* **D76**, 073012 (2007), 0707.1723.
- [30] R. Gandhi, P. Ghoshal, S. Goswami, and S. U. Sankar, *Phys. Rev.* **D78**, 073001 (2008), 0807.2759.
- [31] V. Barger, R. Gandhi, P. Ghoshal, S. Goswami, D. Marfatia, S. Prakash, S. K. Raut, and S. U. Sankar, *Phys. Rev. Lett.* **109**, 091801 (2012), 1203.6012.
- [32] M. Blennow and T. Schwetz, *JHEP* **08**, 058 (2012), [Erratum: *JHEP*11,098(2012)], 1203.3388.
- [33] A. Ghosh, T. Thakore, and S. Choubey, *JHEP* **04**, 009 (2013), 1212.1305.
- [34] A. Ghosh and S. Choubey, *JHEP* **10**, 174 (2013), 1306.1423.
- [35] M. M. Devi, T. Thakore, S. K. Agarwalla, and A. Dighe, *JHEP* **10**, 189 (2014), 1406.3689.
- [36] M. Blennow and T. Schwetz, *JHEP* **09**, 089 (2013), 1306.3988.
- [37] W. Winter, *Phys. Rev.* **D88**, 013013 (2013), 1305.5539.
- [38] S.-F. Ge and K. Hagiwara, *JHEP* **09**, 024 (2014), 1312.0457.
- [39] S. Choubey and P. Roy, *Phys. Rev.* **D73**, 013006 (2006), hep-ph/0509197.
- [40] D. Indumathi, M. V. N. Murthy, G. Rajasekaran, and N. Sinha, *Phys. Rev.* **D74**, 053004 (2006), hep-ph/0603264.

- [41] A. Samanta and A. Yu. Smirnov, *JHEP* **07**, 048 (2011), 1012.0360.
- [42] S. Choubey and A. Ghosh, *JHEP* **11**, 166 (2013), 1309.5760.
- [43] O. L. G. Peres and A. Yu. Smirnov, *Nucl. Phys.* **B680**, 479 (2004), hep-ph/0309312.
- [44] E. K. Akhmedov, M. Maltoni, and A. Yu. Smirnov, *JHEP* **06**, 072 (2008), 0804.1466.
- [45] M. Ghosh, P. Ghoshal, S. Goswami, and S. K. Raut, *Nucl. Phys.* **B884**, 274 (2014), 1401.7243.
- [46] M. Ghosh, P. Ghoshal, S. Goswami, N. Nath, and S. K. Raut, *Phys. Rev.* **D93**, 013013 (2016), 1504.06283.
- [47] J. Valle, *Phys. Lett.* **B199**, 432 (1987).
- [48] M. Guzzo, A. Masiero, and S. Petcov, *Phys. Lett.* **B260**, 154 (1991).
- [49] E. Roulet, *Phys. Rev.* **D44**, 935 (1991).
- [50] Y. Grossman, *Phys. Lett.* **B359**, 141 (1995), hep-ph/9507344.
- [51] C. Biggio, M. Blennow, and E. Fernández-Martínez, *JHEP* **08**, 090 (2009), 0907.0097.
- [52] G. Mitsuka et al. (Super-Kamiokande Collaboration), *Phys. Rev.* **D84**, 113008 (2011), 1109.1889.
- [53] T. Ohlsson, *Rept. Prog. Phys.* **76**, 044201 (2013), 1209.2710.
- [54] N. Fornengo, M. Maltoni, R. Tomàs, and J. Valle, *Phys. Rev.* **D65**, 013010 (2002), hep-ph/0108043.
- [55] M. Gonzalez-Garcia and M. Maltoni, *Phys. Rev.* **D70**, 033010 (2004), hep-ph/0404085.
- [56] A. Friedland, C. Lunardini, and M. Maltoni, *Phys. Rev.* **D70**, 111301 (2004), hep-ph/0408264.
- [57] A. Friedland and C. Lunardini, *Phys. Rev.* **D72**, 053009 (2005), hep-ph/0506143.
- [58] M. Gonzalez-Garcia, M. Maltoni, and J. Salvado, *JHEP* **05**, 075 (2011), 1103.4365.
- [59] F. Escrihuela, M. Tórtola, J. Valle, and O. Miranda, *Phys. Rev.* **D83**, 093002 (2011), 1103.1366.
- [60] T. Ohlsson, H. Zhang, and S. Zhou, *Phys. Rev.* **D88**, 013001 (2013), 1303.6130.
- [61] A. Esmaili and A. Y. Smirnov, *JHEP* **06**, 026 (2013), 1304.1042.
- [62] S. Choubey and T. Ohlsson, *Phys. Lett.* **B739**, 357 (2014), 1410.0410.
- [63] I. Mocioiu and W. Wright, *Nucl. Phys.* **B893**, 376 (2015), 1410.6193.
- [64] A. Chatterjee, P. Mehta, D. Choudhury, and R. Gandhi (2014), 1409.8472.
- [65] S. Fukasawa and O. Yasuda, *Adv. High Energy Phys.* **2015**, 820941 (2015), 1503.08056.
- [66] S. Choubey, A. Ghosh, T. Ohlsson, and D. Tiwari, *JHEP* **12**, 126 (2015), 1507.02211.
- [67] J. Kopp, M. Lindner, T. Ota, and J. Sato, *Phys. Rev.* **D77**, 013007 (2008), 0708.0152.

- [68] C. Athanassopoulos et al. (LSND), Phys. Rev. Lett. **77**, 3082 (1996), nucl-ex/9605003.
- [69] A. A. Aguilar-Arevalo et al. (MiniBooNE), Phys. Rev. Lett. **110**, 161801 (2013), 1207.4809.
- [70] P. Huber, Phys. Rev. **C84**, 024617 (2011), [Erratum: Phys. Rev.C85,029901(2012)], 1106.0687.
- [71] G. Mention, M. Fechner, T. Lasserre, T. A. Mueller, D. Lhuillier, M. Cribier, and A. Le-tourneau, Phys. Rev. **D83**, 073006 (2011), 1101.2755.
- [72] K. Abe et al. (Super-Kamiokande), Phys. Rev. **D91**, 052019 (2015), 1410.2008.
- [73] H. Nunokawa, O. L. G. Peres, and R. Zukanovich Funchal, Phys. Lett. **B562**, 279 (2003), hep-ph/0302039.
- [74] S. Choubey, JHEP **12**, 014 (2007), 0709.1937.
- [75] S. Razzaque and A. Yu. Smirnov, JHEP **07**, 084 (2011), 1104.1390.
- [76] V. Barger, Y. Gao, and D. Marfatia, Phys. Rev. **D85**, 011302 (2012), 1109.5748.
- [77] S. Razzaque and A. Yu. Smirnov, Phys. Rev. **D85**, 093010 (2012), 1203.5406.
- [78] A. Esmaili, F. Halzen, and O. L. G. Peres, JCAP **1211**, 041 (2012), 1206.6903.
- [79] A. Esmaili and A. Yu. Smirnov, JHEP **12**, 014 (2013), 1307.6824.
- [80] M. Lindner, W. Rodejohann, and X.-J. Xu, JHEP **01**, 124 (2016), 1510.00666.
- [81] V. A. Kostelecky and M. Mewes, Phys. Rev. **D70**, 031902 (2004), hep-ph/0308300.
- [82] V. A. Kostelecky and M. Mewes, Phys. Rev. **D69**, 016005 (2004), hep-ph/0309025.
- [83] A. Chatterjee, R. Gandhi, and J. Singh, JHEP **06**, 045 (2014), 1402.6265.